Visualizing Invariant Manifolds in Area-Preserving Maps

Xavier Tricoche, Christoph Garth, Allen Sanderson and Ken Joy

Abstract Area-preserving maps arise in the study of conservative dynamical systems describing a wide variety of physical phenomena, from the rotation of planets to the dynamics of a fluid. The visual inspection of these maps reveals a remarkable topological picture in which invariant manifolds form the fractal geometric scaffold of both quasi-periodic and chaotic regions. We discuss in this paper the visualization of such maps built upon these invariant manifolds. This approach is in stark contrast with the discrete Poincare plots that are typically used for the visual inspection of maps. We propose to that end several modified definitions of the finite-time Lyapunov exponents that we apply to reveal the underlying structure of the dynamics. We examine the impact of various parameters and the numerical aspects that pertain to the implementation of this method. We apply our technique to a standard analytical example and to a numerical simulation of magnetic confinement in a fusion reactor. In both cases our simple method is able to reveal salient structures across spatial scales and to yield expressive images across application domains.

1 Introduction

The Hamiltonian description of dynamical systems, and the formalism arising from it, applies to a large number of natural phenomena from areas as diverse as quantum mechanics, orbital mechanics, fluid dynamics, molecular dynamics, and ecology. At the heart of the Hamiltonian formalism is the principle of *stationary action*, stating that a single scalar function – the *Hamiltonian* – entirely dictates the evolution of a system. In this context, so-called *maps* that describe successive discrete states of an evolving dynamical system and that are used to analyze its structure, can be show to have the property of area preservation, and are extremely rich in structure. From the point of view of scientific visualization, area-preserving maps are simultaneously fascinating and difficult to study as the exhibit fractal topological structure and regions of chaotic behavior.

Xavier Tricoche
Purdue University, West Lafayette, IN 47907, USA, e-mail: xmt@purdue.edu

Christoph Garth, Ken Joy
University of California Davis, Davis, CA 95616 e-mail: cgarth,joy@ucdavis.edu

Allen Sanderson
University of Utah, Salt Lake City, UT 84112 e-mail: allen@sci.utah.edu

Due to the widespread prevalence of Hamiltonian systems in applications, an interest in reliable analysis and visualization of area-preserving maps, needed to obtain insight into the fundamental nature of the described system, is found in many scientific disciplines. However, the intrinsic complexity of such maps makes their analysis challenging. So-called *puncture plots* – direct depictions of map iterates in Poincaré sections – offer a straightforward means to obtain a rough picture of the topological features, but are very limited in their ability to offer a reliable picture of the main structures. Moreover, puncture plots are not a reliable tool to discover a priori unknown structures, and inferring the topology of a system from such plots is typically challenging. Despite the introduction of several techniques to address these shortcomings, the effective analysis of maps remains a difficult task.

We present in this paper a new method for the effective visualization of the main topological structures present in area preserving maps. Specifically, we apply in this setting the concept of finite-time Lyapunov exponent to reveal the invariant manifolds of the topology that form the key geometric structure of the map. Our method offers a clear picture of the island chains, which are the signature of these maps and permits to monitor their qualitative evolution over the course of a time-dependent phenomenon.

We apply our approach to a practical scenario and show its application to a numerical simulation of magnetic confinement in a *Tokamak* fusion reactor. It is important to note that we restrict our considerations to *near-integrable systems*. In other words our method is not meant to process fully stochastic systems. The basic premise of our method is that the most significant features of the map can be captured through relatively simple geometry, an assumption that is no longer valid if the system is dominated by chaos. In fact, from a practical standpoint (e.g., in *magneto-hydrodynamics* (MHD) simulations), the ability to characterize topological transformations in the early stages of the simulation is key since it provides a crucial insight into the long term evolution of the system (loss of stability, loss of confinement, etc.). It is worthwhile to point out however that even in seemingly fully ergodic regions, structures can be identified that control the apparently random behavior of the system.

The contents of this paper are organized as follows. Basic definitions and theoretical results relevant to the presentation of our method are first introduced in Section 2. We then briefly review previous work on map visualization and analysis in Section 3 before describing the algorithmic details of our new method in Section 4. Results are presented in Section 5. Specifically, we consider the important special cases of the *standard map* (Section 5.1) before commenting on our experience with Tokamak simulation data in Section 5.2. Finally conclusion and future research directions are discussed in Section 6.

2 Theoretical and Numerical Foundations

Hamiltonian systems have received considerable attention in mathematics, physics, and computational science. We summarize hereafter key theoretical results. The interested reader is here referred to excellent classical references [15, 20].

2.1 Hamiltonian systems and area-preserving maps

Many systems of mechanics (and optics) can be described by a simple set of ordinary differential equations, known as Hamilton's equations,

$$\frac{dq_i}{dt} = \frac{\partial H}{\partial p_i} \qquad , \qquad \frac{dp_i}{dt} = -\frac{\partial H}{\partial q_i}. \tag{1}$$

The *state* of the system is entirely described by the point $\mathbf{z}(t) = (p_1, \ldots, p_N, q_1, \ldots, q_N)$, in the $2N$-dimensional *phase space*. The p_i are the *momenta*, q_i are the *positions*, and the (scalar) function $H(\mathbf{p}, \mathbf{q}, t)$ is called the *Hamiltonian*. In physical systems, the latter typically describes the total energy of the system.

Expressing the evolution of the system in terms of a general autonomous ordinary differential equation (ODE) initial value problem:

$$\frac{d\mathbf{z}}{dt} = \mathbf{f}(z), \ \mathbf{z}(0) = \mathbf{z_0}, \tag{2}$$

whose solution we denote by $\mathbf{z}(t, \mathbf{z}_0)$, we can define its associated *flow map* $\{\phi_t\}_{t \in \mathbb{R}}$

$$\phi_t(\mathbf{z}_0) := \mathbf{z}(t, \mathbf{z}_0), \ \phi_0(\mathbf{z}_0) \equiv \mathbf{z_0}. \tag{3}$$

The flow map describes the mapping induced by the dynamical system. Equivalent to Equation 1, the *variational principle*, or principle of least action, states that the flow map is constrained to curves, $\mathscr{C}$, in phase space along which the *action integral*: $\int_{\mathscr{C}} \mathbf{p} \cdot d\mathbf{q} - H dt$ is maximized. If the Hamiltonian H itself is an invariant of the motion, the system is said to be conservative.

The *Poincaré map* is a fundamental tool in the study of dynamical systems exhibiting periodicity. In a Hamiltonian system with two degrees of freedom (*i.e.,* $\mathbf{z} = (p_1, p_2, q_1, q_2)$, a case that covers the application scenarios considered in this work) we first observe that for a given value of the Hamiltonian $H = E$, we can express one of the variables in terms of the others, say $p_2 = p_2(p_1, q_1, q_2, E)$, and study the system in a 3D coordinate system (p_1, q_1, q_2), where the motion is confined to a doughnut-shaped *invariant torus* also known as *energy surface*. We then construct the Poincaré map by first selecting a Poincaré section Π, that is a plane transverse (*i.e.,* nowhere tangent) to the flow, say $\Pi = \{q_2 = 0\}$. A point on the plane is therefore described by its coordinates $\mathbf{x}(x, y) := (p_1, q_1)$. By following the trajectory from this point, we define the Poincaré or return map, $\mathscr{P}$, via $\tilde{\mathbf{x}} = \mathscr{P}(\mathbf{x})$, where $\tilde{\mathbf{x}}$ is the

first intersection of the trajectory emanating from **x** and the plane Π, see Figure 1. Observe that the fact that the trajectories return to a vicinity of the starting point (*quasi-periodic* behavior) is a consequence of the fact that the energy surface is bounded.
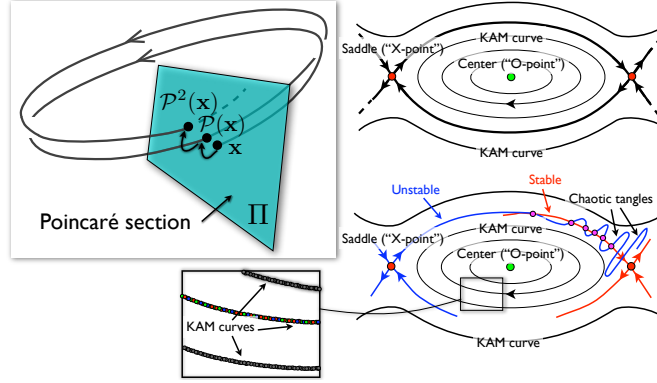

Fig. 1 **Top left:** Two iterations of a Poincaré map. **Right:** Islands of resonance. **Top:** Integrable case. Separatrices connect saddle points in Poincaré map, forming the boundary of an island containing a center point. **Bottom:** Chaotic case. The connections are replaced by the intersection of stable and unstable manifolds forming the tangles that characterize chaos. Quasi-periodic orbits exist both inside and outside of the island and densely populate KAM manifolds (bottom left).

An essential property of Hamiltonian systems compared to other dynamical systems is that the volume of a transported region of the phase space is preserved by the flow map. As a consequence, the Poincaré map itself is *area-preserving* and the vector field describing the transport associated with the map is *divergence-free* [22]. From an algorithmic standpoint this has important implications since typical low-order piecewise polynomial reconstructions of the vector field will in general not preserve this property. We further discuss this problem in Section 2.3 below and provide corresponding results in Section 5.

2.2 Integrable, ergodic and chaotic motion

The simplest picture exhibited by Hamiltonian systems corresponds to the so-called *integrable* case, in which the motion is completely ordered: the orbits $\mathbf{z}(.,\mathbf{z}_0)$ are either closed (and therefore periodic) or they are confined to tori that are invariant under the flow map. In the Poincaré section these tori appear as nested closed curves.

In the opposite limit of *ergodic* behavior the motion is essentially random. In contrast, *chaotic* systems are neither completely integrable nor completely ergodic. Chaotic systems are typical in practice and the primary challenge posed by their analysis is to understand how the structure of phase space progressively "breaks" as

the system deviates from integrability. In particular, so-called islands progressively form in the phase portrait in which a locally linear motion develops. Further, irregular trajectories emerge that wander across circumscribed regions of phase space called *ergodic sea*. Their motion is such that they come arbitrarily close to any position within those regions. In the following, we limit our description to the two-dimensional case; however, equivalent definitions apply to N-dimensional systems.

2.2.1 Periodic orbits and linearized motion

Periodic orbits of the system form fixed points of the Poincaré map. A periodic orbit of period p is invariant under p iterations of the Poincaré map: $\mathscr{P}^p(\mathbf{x_0}) := \mathscr{P}(\mathscr{P}^{p-1}(\mathbf{x_0})) = \mathbf{x_0}$, where p is the smallest integer that satisfies this relation. We refer to $\mathbf{x_0}$ as a fixed point of period p. The type of a fixed point can be determined by a local linear analysis of the Poincaré map in its vicinity. More precisely, a linear approximation of the local motion about $\mathbf{x_0}$ is based on the Jacobian $\mathbf{J}_p := \nabla_{\mathbf{x}} \mathscr{P}^p$ and the eigenvalues λ_i, $i = \{1,2\}$ of $\mathbf{J}_p$ determine the nature of the fixed point. If they are complex conjugates the Poincaré map displays elliptical motion under the mapping near the fixed point. This "O-point" configuration is called *center* in the visualization literature [12]. A local *island* of dominantly regular motion will exist (Figure 1, top right). If the eigenvalues are real and of opposite sign, $\mathbf{x_0}$ forms a *saddle* (or "X-point") and the eigenvector of $\mathbf{J}_p$ associated with the negative (resp. positive) eigenvalue aligns with the *stable* (resp. *unstable*) *manifolds* of $\mathbf{x_0}$. These manifolds form the boundary of the islands and are the *separatrices* of the topology. Saddle points (and the associated unstable orbit) lie at the heart of chaos. In general stable and unstable manifolds intersect in patterns called *chaotic tangles*, and their structure dominates the dynamics in the chaotic sea, see Figure 1, bottom right.

2.2.2 Quasi-periodic orbits and KAM theory

Beside fixed points, islands, and ergodic seas, the Poincaré map exhibits curves that are densely covered by quasi-periodic orbits. The period of these orbits is therefore *irrational* and the fundamental KAM theorem [13, 1, 23] states that those manifolds (so-called *KAM surfaces*) that have "sufficiently irrational" periods will survive the onset of chaos through nonlinear perturbations. The KAM surfaces form perfect barriers to transport in the phase portrait, hence their crucial importance in confinement problems. As chaos increases these surfaces are progressively destroyed and replaced by so-called *Cantor sets*, which offer only partial barrier to transport.

2.3 Numerical Aspects

The analysis of an area preserving map depends heavily on an accurate and efficient integration of the flow map $\phi_{t\,t\in\mathbb{R}}$. This computation yields the successive iterates

of the Poincaré map $\mathscr{P}^i, i \in \{1,..,N\}$. An exception to this rule are discrete analytical maps where an explicit formula $\mathbf{f}$ describes the relationship $\mathbf{x}_{n+1} = \mathbf{f}(\mathbf{x_n})$. We consider one such map in Section 5.1. In general, however, the computation of the Poincaré map is made challenging by the need to maintain long term accuracy in the numerical integration of an ODE. In the context of Hamiltonian systems in particular, the property of area-preservation is essentially impossible to guarantee through conventional integration schemes such as Runge-Kutta methods [19]. So-called geometric (or symplectic) integrators do explicitly enforce the invariance of these properties along the integration [7]. However, their application requires a specific formulation of the dynamics (*e.g.,* an explicit expression for the Hamiltonian of the problem), which is rarely available in numerical simulations. When processing such datasets, the continuous reconstruction of the field through piecewise polynomial functions is not exactly conservative. In this case, the area-preserving property is a theoretical reference for the behavior of the studied phenomenon rather than a numerical reality. For this work, we applied the divergence cleaning approach based on *Hodge projection* advocated by Peikert and Sadlo [24]. However we found the overhead caused by the additional piecewise linear divergence-free interpolation they proposed to outweigh the accuracy benefit. Practically, we used in this work the classic Runge-Kutta triple Dormand-Prince DP6(5) method [26] whose dense output provides an excellent balance of accuracy and speed. However, we found it necessary to require very low relative tolerance of the integration scheme ($\varepsilon = 10^{-8}$) in order to achieve satisfactory results.

3 Previous Work

While discrete dynamical systems and area-preserving maps are not commonly addressed in visualization publications, a number of previous contributions provide the foundations of our method. We briefly summarize them next.

The topological approach has been introduced in visualization by Helman and Hesselink [11] who first showed that the topological skeleton offers a schematic and insightful picture of a (continuous) flow. Numerous contributions have since been made to that general methodology and it remains an active research area [32, 9, 10]. Closer to the topic of this paper, Löffelmann et al. proposed several methods for the intuitive visualization of discrete dynamical systems defined analytically [18, 16, 17]. In particular, these authors devised representations that aim at revealing the continuous structures underlying the map. Most recently, Peikert and Sadlo applied a Poincaré map approach to the visualization of vortex rings in a flow recirculation bubble [24, 25]. While the resulting map is not strictly area-preserving, they showed that the topological structures that arise in this context are fundamentally similar. Therefore, they proposed an image-based method to visualize the separatrices that originate from the saddle points located at each extremity of the recirculation bubble and used them to reveal the convoluted patterns formed by their successive intersections along with the associated island chains and stochastic behavior. They also

described an iterative scheme to compute the *O-points* located in each of the main islands by successive approximation of the location rotation pattern of the map.

Hamiltonian maps have also been studied in the artificial intelligence and data mining. In his Ph.D. thesis, Yip developed a computer system (called *KAM*) [34] that combines geometric and graph theory criteria commonly used in artificial intelligence to automatic identify the three main types of orbits present in a map: closed loop, island chain, and separatrix. Following a similar approach, Bagherjeiran and Kamath applied a data mining approach to identify patterns in Poincaré plots [2]. Practically, a minimum spanning tree followed by a clustering step is used to infer the 1-dimensional structure of a series of puncture points. Both of these approaches are best suited for the detection of rather large structures of the map. Additionally they do not provide the explicit boundaries of the structures but rather aim at detecting the main features.

In the specific context of fusion reactor simulations, which we consider in Section 5.2, Sanderson et al. recently presented a method that automatically constructs a geometric approximation of 1-manifolds in Poincaré maps by resolving the connectivity of the discrete plot [30]. Note that this technique does not explicitly identify invariant manifolds of the topology but instead focuses on the irrational (KAM) surfaces sampled by the seeding. The available curve geometry can then be leveraged to approximate the location of the O-points [31, 25]. The visualization is constructed by probing the map at a discrete set of locations and takes advantage of inherent symmetries in the Tokamak.

Finally, researchers in physics and applied mathematics have considered maps from an algorithmic perspective. England et al. recently proposed a method to construct stable and unstable manifolds in Poincaré maps from saddle points by successively extending the piece of manifold that has already been computed [3]. Again, a similar approach was used in [25]. Levnajić and Mezić considered the application of the ergodic partition theory to the visualization of the standard map [14], whereby their method yields an image in which a piecewise constant color plot reveals coherent regions of the phase space. Most germane to the ideas presented in this paper is the work carried out simultaneously by Grasso et al. [6] who applied FTLE and LCS (Section 4) to identify transport barriers in magnetic fields used in plasma confinement. We concentrate hereafter on the visualization implications of this approach and study in more detail the relationship of LCS with the underlying fractal topology.

4 Proposed Approach

We saw in Section 2 that the structure of Poincaré maps in Hamiltonian systems can be readily described in topological terms. Hence, it would seem natural to resort to the algorithmic framework of topological methods to create insightful representations of these systems. Unfortunately, this approach proves fantastically difficult in the context of numerical data. Indeed, finding the fixed points of the map is a chal-

lenging task that requires a very dense and expensive sampling of the phase portrait. Once fixed points have been identified the next hurdle consists in characterizing the linear type of the fixed point which requires to compute the associated Jacobian. Estimating this derivative properly is also challenging given the chaotic behavior that is unavoidably present in the vicinity of hyperbolic (saddle) points. Finally, the construction of the invariant manifolds associated with the saddles is problematic from a numerical standpoint since topologically they correspond to homoclinic or heteroclinic connections that are known to be generically unstable.

We therefore propose to capture these manifolds in a numerically robust way through the computation of the finite-time Lyapunov exponent (FTLE) in these maps. By yielding an image in which separatrices of the topology are revealed as ridges of the FTLE field this approach provides a powerful means to identify salient geometric structure in a period-agnostic way.

4.1 Finite-time Lyapunov exponent

Haller in his seminal work [8] popularized the concept of finite-time Lyapunov exponent to the engineering and visualization community by defining *Lagrangian coherent structures* (LCS) as ridges of the FTLE. Following his approach, unstable (resp. stable) invariant manifolds are characterized as height ridges of FTLE in forward (resp. backward) direction.

Practically, one considers at instant t_0 the flow map $\mathbf{x}_T$, whereby $T = t_0 + \tau$ and τ is the time interval considered for the flow transport. The variations of this flow map around a given position $\mathbf{x_0}$ are determined by its Jacobian $J_{\mathbf{x}}(t,t_0,\mathbf{x_0}) := \nabla_{\mathbf{x_0}}\mathbf{x}(t,t_0,\mathbf{x_0})$ at $\mathbf{x_0}$ and the maximal rate of dispersion of particles located around $\mathbf{x_0}$ at t_0 is given by following expression ($\lambda_{\max}$ designates the largest eigenvalue):

$$\sigma_\tau(t_0,\mathbf{x_0}) := \sqrt{\lambda_{\max}(J_{\mathbf{x}}(t,t_0,\mathbf{x_0})^T J_{\mathbf{x}}(t,t_0,\mathbf{x_0}))}.$$

The average exponential separation rate $\lambda(t,t_0,\mathbf{x_0})$, for positive or negative τ, is then called finite-time Lyapunov exponent and defined [8] as

$$\lambda(t,t_0,\mathbf{x_0}) = \frac{1}{|\tau|}\log\,\sigma_\tau(t_0,\mathbf{x_0}).$$

Ridges of λ for forward (resp. backward) advection correspond to unstable (resp. stable) manifolds that strongly repel (resp. attract) nearby particles. Note that this technique has attracted a significant interest in the visualization literature in recent years [4, 28, 27, 5, 33, 29].

It is important to note that, in the presence of a canonical reference frame, these ridges typically capture the separatrices of the topology of steady vector fields [8], owing to the hyperbolicity of the trajectories in the vicinity of the separatrices. Hence the FTLE approach offers a promising alternative to the standard topolog-

ical method to study the salient structures exhibited by area-preserving maps. In addition, the FTLE method is more robust to noise since it defines structures as the ridge surfaces of a continuously varying coherence measure. Therefore it automatically quantifies the *fuzziness* of the extracted manifolds in the context of chaotic motion. Algorithmic and numerical aspects of this strategy are discussed next.

4.2 Computing FTLE in maps

A first problem when trying to extend the definition of FTLE in maps is the discrete nature of the dynamics that they describe. Indeed, the notion of finite-time must be expressed in a setup where time is, at best, a discrete notion. Note that in the context of the magnetic field considered in Section 5.2, the (integration) time is also available as a continuous dimension. However it makes more sense from a physical standpoint and for the sake of the corresponding analysis to consider the discrete time associated at each particle with complete revolutions around the system.

The problem posed by discrete time can be solved by defining FTLE at a given location $\mathbf{x_0}$ as:

$$\lambda(k, 0, \mathbf{x_0}) = \frac{1}{|k|} \log \sigma_k(0, \mathbf{x_0}), \text{ with } k \in I\!N.$$

In other word, one replaces time by a number of iterations of the map in the previous definition of FTLE. However, when the map is derived from a continuous system, this definition amounts to a reparameterization of the orbits of the system such that all trajectories complete a full revolution in constant and uniform time. This transformation is a standard procedure in the study of Hamiltonian dynamics where it leads to so-called systems with one and a half degrees of freedom [22].

Another difficulty consists in identifying a proper time scale (τ or k) for the characterization of the structures. While this problem is inherently associated with Haller's FTLE definition it is particularly salient in the case of maps because the fractal complexity of the topology leads to manifolds whose associated time scales vary dramatically across the phase portrait. To tackle this problem we experimented with several approaches. The first one simply consists in integrating the map for a large enough number of iterations to "sharpen" even the small (visible) structures. A clear downside of this approach is that the structures associated with a shorter "time" scale (typically the larger ones) become extremely noisy in the resulting images as aliasing becomes pronounced in their vicinity. An alternative solution consists in computing a FTLE image for each step of a large number of iterations and applying some image processing technique on the resulting stack of image to obtain the best feature characterization. This approach shares some conceptual similarities with the notion of scale space whereby here the the number of map iterations forms a discrete scale axis. A simple such operation consists in identifying at each pixel of the created map the value k such that some image quality metric is maximized. Examples include the value of FTLE or the corresponding ridge strength. Unfortunately this approach provides no guarantee to yield a spatially coherent (e.g., smooth) scale

picture since the decision is made on a per-pixel basis. The other shortcoming of this solution is that it requires a large number of intermediate images to be stored as the total number of iterations of the map is computed in order to offer a fine enough sampling of the scale axis. Overall this approach offered some disappointing results although it seems worthwhile to investigate further in future work. We compare the results of these various approaches in Section 5.

5 Results

We present in this section results obtained for an analytical and a numerical dataset, respectively. In each case, the computed FTLE values are displayed using a color map that was previously described in [5]. Its basic idea is to favor a clear distinction between stable and unstable hyperbolic behavior through a distinction between blue and red colors while encoding the relative strength of this behavior through the brightness of the color (stronger values yield darker colors). Aliasing issues caused by the fractal nature of the topology are addressed through smooth downsampling of high resolution maps. The computation of both flow map and FTLE is carried out in on a 32-core Intel "Nehalem" machine, leveraging the embarrassingly parallel nature of the problem. Note that we also implemented the method on the GPU but found the limited accuracy in this case to be unsuitable for our purpose.

5.1 Standard Map

The standard map (also known as *Chirikov-Taylor map*) is an area-preserving 2D map of the 2π square onto itself defined as follows:

$$p_{n+1} = p_n + K\sin(\theta_n) \tag{4}$$
$$\theta_{n+1} = \theta_n + p_{n+1}, \tag{5}$$

whereby p_n and θ_n are taken modulo 2π. K is a parameter that controls the nonlinearity of the map. The standard map describes the dynamics of several mechanical systems and has attracted the attention of theoretical and computational research alike since it is a simple yet powerful tool to study Hamiltonian chaos. This map allows us to test our proposed method across a range of configurations.

Figure 2, left, shows the invariant manifolds of the standard map with $K = 0.7$ as computed for 50 iterations of the map. It can be seen that the FTLE-based visualization clearly reveals the individual island chains of the map. A range of spatial scales are present in this representation that confirm the fractal complexity of the topology. Another compelling property of this representation is its ability to convey the chaos that surround the saddle points of the map. In particular, the saddle of period 1, visible at the top and bottom of the domain (by periodicity) exhibit a typical picture

of chaotic tangle. Similarly, this feature is noticeable at both saddles of the period-2 island chain that runs through the middle of the map. These images in fact echo the observations made by Mathur et al. [21] in which an intricate picture of LCS manifolds where shown to underly the apparently chaotic behavior of a turbulent flow.
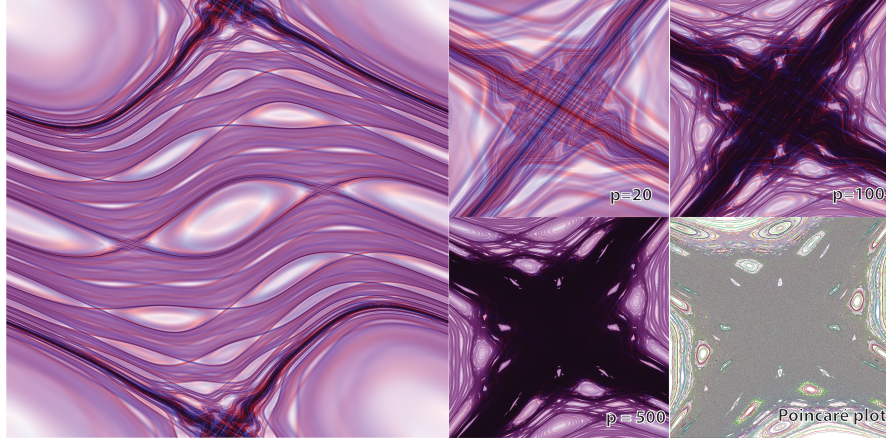

Fig. 2 Left: Topology of the standard map for K=0.7: the map begins to exhibit chaotic regions. Right: Invariant manifolds in the vicinity of the 1-saddle as extracted by our method using varying maximal periods. The chaos visible in the overall image is revealed as the product of chaotic tangles. The increasing maximal period count reveals an increasing number of separatrices that form the chaotic tangle.

The application of this approach to an analytical map offers the opportunity to investigate the fractal nature of the topology at arbitrary resolution, only limited by the machine precision. A close-up view in the vicinity of the saddle point visible at the top and bottom of the previous image is proposed in Figure 2, right, which reveals how subtle structures are properly captured by our method despite their challenging complexity. In particular, the chaotic tangle that is a hallmark of chaos in such systems is prominently present in this image. A comparison with a standard puncture plot offers a contrasting view of these structures.

By increasing the magnification, additional structures become visible, such as those shown in Figure 3. Note that to achieve a dense enough coverage of such a small region of the map, the puncture plot that is shown here for reference requires an extremely high number of iterations, which goes at the expense of the numerical accuracy of the resulting computation.
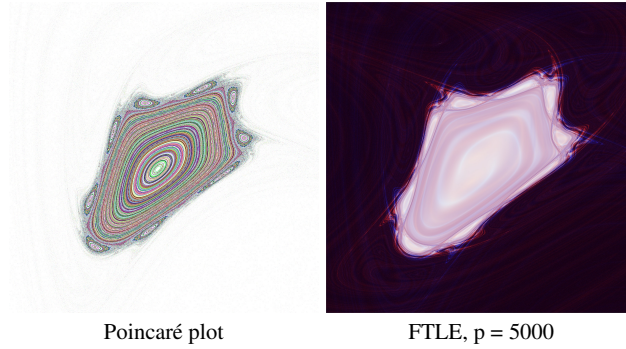
Poincaré plot   FTLE, p = 5000

Fig. 3 500× magnified region of the standard map (K=1.1). The visible island is embedded in the chaotic region, which appears as the region of maximum separation (right image).

5.2 MHD Simulation of Plasma Confinement in a Tokamak Fusion Reactor

Magnetic fusion reactors, such as the International Thermonuclear Experimental Reactor (ITER), a Tokomak reactor scheduled for completion in 2018 will be the source for future low cost power. In their basic operation, magnetic confinement fusion uses the electrical conduction of the burning plasma to contain it within magnetic fields (refer to Figure 1 in Chapter 23).

A critical characteristic of a typical fusion reactor is the growth of instabilities in the plasma due to the large gradients of density and temperature, the field geometry, and the inherent self-consistent interactions between charged particles and electromagnetic waves. Plasma instabilities occur on very different spatial and temporal scales and can represent highly unique phenomena. One such instability, *magnetic reconnection*, prevents the magnetic field from confining the plasma and leads to its transport. Locating these phenomena can best be done through visualizing the topology of the magnetic field and identifying features within it.

In the normal operation of a tokamak reactor, the magnetic field lines are topologically distinct from each other and form a series of concentric flux surfaces that confine the plasma. Because the magnetic field lines are either periodic, quasi-periodic, or chaotic, the topology can clearly be seen by creating a Poincaré plot. In the presence of instabilities, the magnetic field can become distorted and form magnetic islands. It is the formation of the islands that constitutes magnetic reconnection. Locating these features; islands, separatrices, and X points, is an important component in understanding plasma transport in magnetic fusion research. However, generating Poincaré plots is computationally expensive and unless seed points for the plot are selected carefully, features within the magnetic field may be missed. As such developing a robust technique that allows for the rapid visualization and facilitates the analysis of topological structures of magnetic field lines in an automatic fashion will aid in the future design and control of Tokamak reactors.

To analyze this time-dependent dataset we first map the computational mesh to its parametric representation in computational space. This amounts to opening up the mesh in both the poloidal and the toroidal direction to yield a 3D mesh in which two directions are periodic. To illustrate some of the aspects discussed previously we first show in Figure 4 the results obtained in the same dataset for various iterations of the map.
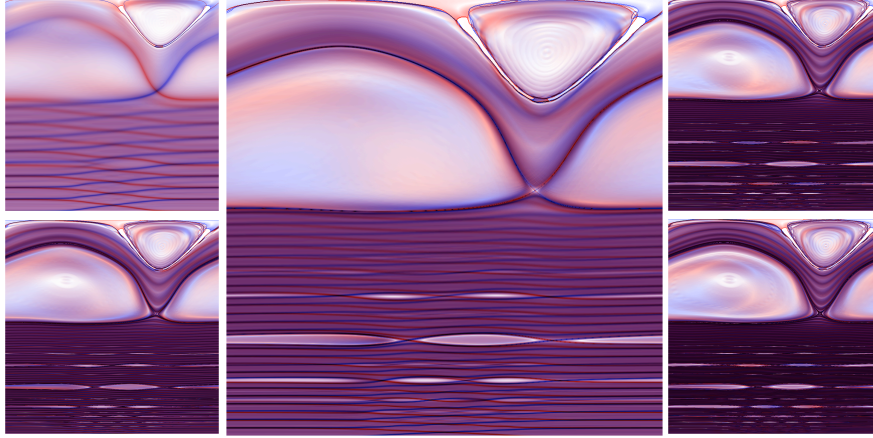

Fig. 4 FTLE mapping of a time step of the Tokamak dataset for various iterations of the map. The central image is obtained for 50 toroidal rotations, while the other ones are obtained for 10, 30, 70 and 100 rotations respectively. The major islands are clearly visible.

It can be seen that increasing the number of iterations yields a picture in which the finest structures exceed the sampling resolution and lead to significant artifact problems. As mentioned previously, selecting in a spatially varying way the best scale to represent the underlying structures given the limited bandwidth of the image is an open problem for which the solutions that we have investigated so far failed to provide satisfactory results. The close relationship between the FTLE picture and the topology of the Poincaré map is confirmed in Figure 5.

The images produced by our method lend themselves to an intuitive navigation of the time axis of the simulation. Figure 6 provides such an illustration of the evolution of the topology. In particular it can be seen that a major topological transformation affects the 1-saddle that is visible in the upper part of the domain. This bifurcation known as *basin bifurcation* induces a dramatic reorganization of the transport in the domain.
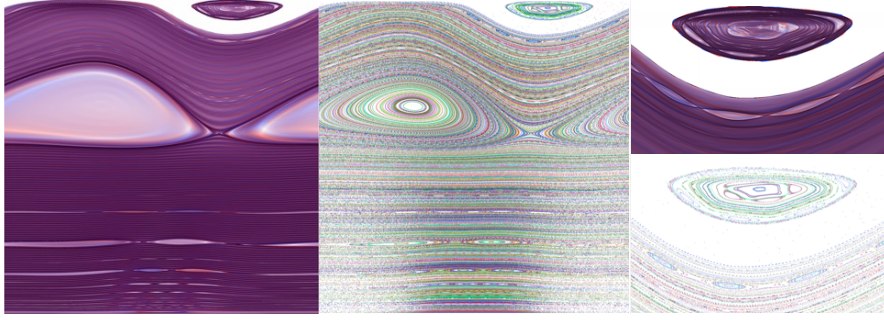
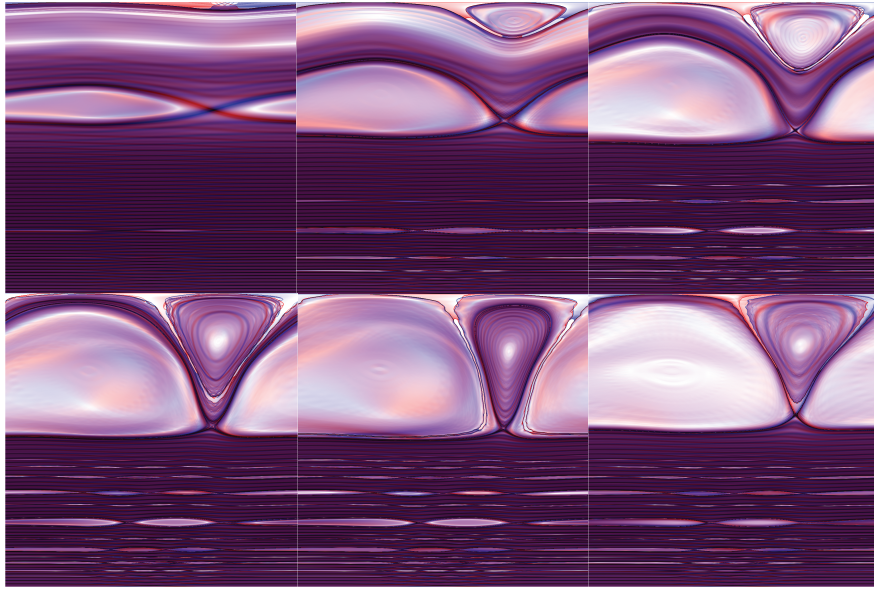**Fig. 5** Comparison between FTLE and Poincaré plot in Tokamak dataset.

Fig. 6 Temporal evolution of the topological structures present in the map (T=500, 1000, 2000, 3000, 4000, 7000). Each image was obtained after 50 iterations of the map.

6 Conclusion

We have presented an algorithmic and computational framework to permit the effective visualization of area-preserving maps associated with Hamiltonian systems. While these maps are of great theoretical interest they are also very important in practice since they offer a geometric interpretation of the structural behavior of complex physical systems. Our method, while conceptually simple and straightforward to implement, significantly improves on previous work by allowing for the identification of very subtle structures that would typically be missed through Poincaré plot investigation of the map. In this context our method successfully addresses one of

the primary difficulty posed by this type of structural analysis, namely the numerical challenge associated with an accurate computation of Poincaré maps, which requires the successive integration of an ordinary differential equation. By restricting our computation to a comparatively small number of iterations of the period from any given point (commensurate with the period range relevant to the analysis) we are able to obtain reliable results that are further enhanced by a robust correction strategy motivated by topological considerations.

We have tested our methods on a standard analytical map and on a numerical simulation of magnetic confinement. Our results underscore the potential of our method to effectively support the offline analysis of large simulation datasets for which they can offer a valuable diagnostic tool. In that regard there are many promising avenues for future work. As pointed out in the paper, a proper characterization of the best period to match the spatial scale of the structures would dramatically enhance the results achieved so far. Of course, computational efficiency is a major concern with this method and although it is embarrassingly parallel, adaptive methods, as such recently proposed in the literature, could greatly increase the efficiency of our implementation. Finally, it would be most definitely interesting to combine such a visualization with an explicit extraction of the topology. In that regard, the images obtained suggest that an image processing approach could directly leverage the extracted information while exploiting the theoretical framework of image analysis to do so in a principled way.

Acknowledgements

References

1. V. I. Arnold. Proof of A. N. Kolmogorov's thereom on the preservation of quasiperiodic motions under small perturbations of the Hamiltonian. *Russ. Math. Surv.*, 18(5):9, 1963.
2. A. Bagherjeiran and C. Kamath. Graph-based methods for orbit classification. In *Proc. of Sixth SIAM International Conference on Data Mining*, April 2006.
3. J. England, B. Krauskopf, and H. Osinga. Computing one-dimensional global manifolds of poincaré maps by continuation. *SIAM Journal of Applied Dynamical Systems*, 4(4):1008–1041, 2005.
4. C. Garth, F. Gerhardt, X. Tricoche, and H. Hagen. Efficient computation and visualization of coherent structures in fluid flow applications. *IEEE Transactions on Visualization and Computer Graphics*, 13(6):1464–1471, 2007.
5. C. Garth, A. Wiebel, X. Tricoche, H. Hagen, and K. Joy. Lagrangian visualization of flow embedded structures. *Computer Graphics Forum*, 27(3):1007–1014, 2008.
6. D. Grasso, D. Borgogno, F. Pegoraro, and T. Schep. Barriers to field line transport in 3d magnetic configurations. *Journal of Physics*, Conference Series 260(012012), 2010.
7. E. Hairer, C. Lubich, and G. Wanner. *Geometric Numerical Integration*. Springer-Verlag, 2006.

8. G. Haller. Distinguished material surfaces and coherent structures in three-dimensional flows. *Physica D*, 149:248–277, 2001.
9. H. Hauser, H. Hagen, and H. Theisel. *Topology Based Methods in Visualization*. Springer, 2007.
10. H.-C. Hege, K. Polthier, and G. Scheuermann. *Topology Based Methods in Visualization II*. Springer, 2009.
11. J. Helman and L. Hesselink. Visualizing vector field topology in fluid flows. *IEEE Computer Graphics and Applications*, 11(3):36–46, 1991.
12. J. L. Helman and L. Hesselink. Visualizing vector field topology in fluid flows. *IEEE Computer Graphics and Applications*, 11(3):36–46, May 1991.
13. A. N. Kolmogorov. On the conservation of conditionally periodic motions under small perturbation of the Hamiltonian. *Dokl. Akad. Nauk. SSR*, 98:469, 1954.
14. Z. Levnajić and I. Mezić. Ergodic theory and visualization. i. mesochronic plots for visualization of ergodic partition and invariant sets. *Chaos*, 20(033114), 2010.
15. A. J. Lichtenberg and M. A. Lieberman. *Regular and Chaotic Dynamics, 2nd ed.* Springer-Verlag, New York, 1992.
16. H. Löffelmann, H. Doleisch, and E. Gröller. Visualizing dynamical systems near critical points. In *14th Spring Conference on Computer Graphics*, pages 175–184, 1998.
17. H. Löffelmann and E. Gröller. Enhancing the visualization of characteristic structures in dynamical systems. In *Visualization in Scientific Computing '98*, pages 59–68, 1998.
18. H. Löffelmann, T. Kucera, and E. Gröller. Visualizing poincaré maps together with the underlying flow. In H.-C. Hege and K. Polthier, editors, *Mathematical Visualization: Proceedings of the International Workshop on Visualization and Mathematics '97*, pages 315–328. Springer, 1997.
19. J. Marsden and M. West. *Discrete Mechanics and Variational Integrators*. Acta Numerica, 2001.
20. J. E. Marsden and T. Ratiu. *Introduction to Mechanics and Symmetry*. Texts in Applied Mathematics vol. 17. Springer-Verlag, 2003.
21. M. Mathur, G. Haller, T. Peacock, J. Ruppert-Felsot, and H. Swinney. Uncovering the lagrangian skeleton of turbulence. *Phys. Rev. Lett.*, 98:144502, 2007.
22. P. Morrison. Magnetic field lines, hamiltonian dynamics, and nontwist systems. *Physics of Plasma*, 7(6):2279–2289, 2000.
23. J. Moser. On invariant curves of area-preserving mappings of an annulus. *Nachr. Akad. Wiss. Göttingen, Math. Phys. Kl. II 1,1*, Kl(1):1, 1962.
24. R. Peikert and F. Sadlo. Visualization Methods for Vortex Rings and Vortex Breakdown Bubbles. In A. Y. K. Museth, T. Möller, editor, *Proceedings of the 9th Eurographics/IEEE VGTC Symposium on Visualization (EuroVis'07)*, pages 211–218, May 2007.
25. R. Peikert and F. Sadlo. Flow Topology Beyond Skeletons: Visualization of Features in Recirculating Flow. In H.-C. Hege, K. Polthier, and G. Scheuermann, editors, *Topology-Based Methods in Visualization II*, pages 145–160. Springer, 2008.
26. P. J. Prince and J. R. Dormand. High order embedded runge-kutta formulae. *Journal of Computational and Applied Mathematics*, 7(1), 1981.
27. F. Sadlo and R. Peikert. Efficient Visualization of Lagrangian Coherent Structures by Filtered AMR Ridge Extraction. *IEEE Transactions on Visualization and Computer Graphics*, 13(5):1456–1463, September-October 2007.
28. F. Sadlo and R. Peikert. Visualizing lagrangian coherent structures: A comparison to vector field topology. In *Topology-Based Methods in Visualization 2007, to appear*, 2007.
29. F. Sadlo and D. Weiskopf. Time-Dependent 2-D Vector Field Topology: An Approach Inspired by Lagrangian Coherent Structures. *Computer Graphics Forum*, 29(1):88–100, 2010.
30. A. Sanderson, G. Cheng, X. Tricoche, D. Pugmire, S. Kruger, and J. Breslau. Analysis of recurrent patterns in toroidal magnetic fields. *IEEE Transactions on Visualization and Computer Graphics*, 16(6):1431–1440, 2010.
31. A. Sanderson, X. Tricoche, C. Garth, S. Kruger, C. Sovinec, E. Held, and J. Breslau. Poster: A geometric approach to visualizing patterns in the poincaré plot of a magnetic field. In *Proc. of IEEE Visualization 06 Conference*, 2006.

32. G. Scheuermann and X. Tricoche. Topological methods in flow visualization. In C. Johnson and C. Hansen, editors, *Visualization Handbook*, pages 341–356. Academic Press, 2004.
33. B. Soni, D. Thompson, and R. Machiraju. Visualizing particle/flow structure interactions in the small bronchial tubes. *IEEE Transactions on Visualization and Computer Graphics*, 14(6):1412–1427, 2008.
34. K. M.-K. Yip. *KAM: A System for Intelligently Guiding Numerical Experimentation by Computer*. MIT Press, 1992.